DOI: 10.1002/chem.200600888

Tris-Cyclometalated Iridium(III) Complexes of Carbazole(fluorenyl)pyridine Ligands: Synthesis, Redox and Photophysical Properties, and Electrophosphorescent Light-Emitting Diodes

Sylvia Bettington,[a] Mustafa Tavasli,[a] Martin R. Bryce,*[a] Andrew Beeby,[a] Hameed Al-Attar,[b] and Andrew P. Monkman*[b]

Abstract: Using ligands synthesized by Suzuki cross-coupling methodology, new phosphorescent homoleptic tris-cyclometalated complexes have been obtained, namely *fac*-[Ir(Cz-2-Fl$_n$Py)$_3$] (**1d–f**) and *fac*-[Ir(Cz-3-Fl$_n$Py)$_3$] (**2d–f**), which are solution-processible triplet emitters (Cz denotes *N*-hexylcarbazole, *n* is the number of 9,9′-dihexylfluorene (Fl) units ($n=0,1,2$) and Py is pyridine). In all cases, Py and Fl are substituted at the 2- and 2,7-positions, respectively, and Cz moieties are substituted by either Py or Fl at the 2- or 3-positions, in series **1** and **2**, respectively. The oxidation potential of **1d** studied by cyclic voltammetry ($E^{ox}_{1/2}=0.14$ V, versus Ag/AgNO$_3$, CH$_2$Cl$_2$) is less positive (i.e. raised HOMO level) compared to that of the isomer **2d** ($E^{ox}_{1/2}=0.30$ V), where the Cz-nitrogen is *meta* to the Ir center. Ligand-centered oxidations occur at more positive potentials, leading to 7+ oxidation states with good chemical reversibility and electrochemical quasi-reversibility, for example, for **2f** $E^{ox}_{pa}=0.45$ (1e), 0.95 (3e), 1.24 V (3e). Striking differences are seen in the solution-state photophysical data between complexes [Ir(Cz-2-Py)$_3$] (**1d**) and [Ir(Cz-3-Py)$_3$] (**2d**), in which the Cz moiety is bonded directly to the metal center: for the latter there is an 85 nm blue-shift in emission, a decrease in the luminescence lifetime and an increase in the PLQY value. Organic light emitting devices were made by spin-coating using polyspirobifluorene:-bis(triphenyl)diamine (PSBF:TAD) copolymer as host and the complexes **1d** or **2d** as dopants. Turn-on voltages are low (3–4 V). With **1d** orange light is emitted at $\lambda_{max}=590$ nm with an EQE of 1.3% (at 7.5 mA cm^{-2}) and an emission intensity (luminance) of 4354 cd m^{-2} (at 267 mA m^{-2}). The green emission from **2d** devices ($\lambda_{max}=500$ nm) is due to the reduced electron-donating ability of the carbazole unit in **2d**. Recording the EL spectra of the **1d** device at 6 V (current density, 100 mA cm^{-2}) established that the time to half brightness was about 9 h under continuous operation with no change in the spectral profile, confirming the high chemical stability of the complex.

Keywords: carbazole · cyclometallation · fluorene · fluorescence · organic light-emitting devices · pyridine

Introduction

Highly conjugated molecules, especially multi-directional architectures, are of great interest as advanced materials.[1] The core unit is generally a multi-functional organic moiety or a coordinated metal center around which the spacial geometry suppresses self-aggregation effects, thus favoring good solubility and affording optoelectronic properties of importance for fundamental studies and for device applications. Homoleptic cyclometalated metal complexes have received only limited attention as cores in π-extended architectures. There is scope to develop new materials of this type as many cyclometalated complexes are both redox-active and highly emissive, especially as their *facial* isomers. A broad selection of ligands, principally based upon 2-phe-

[a] Dr. S. Bettington, Dr. M. Tavasli, Prof. M. R. Bryce, Dr. A. Beeby
Department of Chemistry
Durham University
Durham DH1 3LE (UK)
Fax: (+44) 191-384-4737
E-mail: m.r.bryce@durham.ac.uk

[b] Dr. H. Al-Attar, Prof. A. P. Monkman
Department of Physics
Durham University
Durham DH1 3LE (UK)
Fax: (+44) 191-334-5823
E-mail: a.p.monkman@durham.ac.uk

Supporting information for this article is available on the WWW under http://www.chemistry.org or from the author.

nylpyridine,[2] have been utilized to form phosphorescent bis-[3] and tris-cyclometalated[4] iridium(III) complexes. The photophysical properties of these phosphors can, to some extent, be tuned by varying the ligand[5] or its substituent groups and also by the use of additional ancillary ligands.[6] Many such complexes serve as active components in electrophosphorescent organic/polymer light emitting devices (O/PLEDs) where they are normally used as an emitting guest in a blend with a host material.[7] Mixing of the electrogenerated singlet and triplet excited states by intersystem crossing removes the spin-forbidden nature of the radiative relaxation of the triplet excited state so singlet and triplet excited states both contribute to light emission. Additionally, the triplet state lifetime is shortened, thereby suppressing triplet-triplet annihilation. Solution processing techniques offer a simple route for device fabrication.[8]

We were attracted by the prospect of incorporating carbazole units into the ligands of cyclometalated complexes, including π-extended systems. Carbazole-containing linear conjugated oligomers and polymers are important in organic materials chemistry due to their high stability, processability and the hole-transporting properties of the carbazole unit: examples include 3,6-carbazole-benzo-2,1,3-thiadiazole copolymers,[9] 2,7-carbazolenevinylene systems and fused-ring derivatives (e.g. diindolocarbazoles).[10] There are recent reports of emissive carbazole-fluorene co-oligomers and polymers,[11] and cyclometalated iridium complexes with attached carbazole units,[12] including phenylcarbazole dendrons.[13]

Our targets were two new series of conjugated carbazole-(fluorenyl)pyridine ligands: Cz-2-Fl$_n$Py (**1a–c**) and Cz-3-Fl$_n$Py (**2a–c**), where the *N*-hexylcarbazole (Cz) moiety is substituted at the C-2 and C-3 positions by the fluorene (Fl) ($n=1$, 2) or pyridine (Py) unit, respectively.

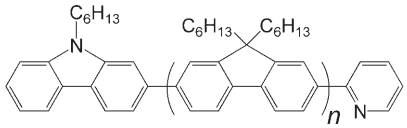

Series 1: Cz-2-Fl$_n$Py: **1a-c**

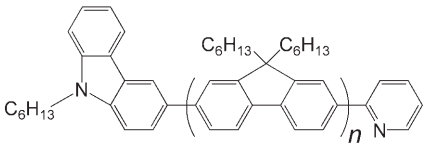

Series 2: Cz-3-Fl$_n$Py: **2a-c**

a (n = 0), **b** (n = 1), **c** (n = 2)

The six new triply cyclometalated iridium(III) complexes **1d–f** and **2d–f** were synthesized to study their optoelectronic properties. Complexes **1d** and **2d** are very rare examples of iridium(III) systems where the metal is directly bonded to a carbazole unit[14] and we are not aware of any previous examples of triply cyclometalated carbazole-containing systems. A comparison of the iridium(III) complexes in series **1** (2-substituted carbazole) and series **2** (3-substituted carbazole) has provided a unique opportunity to probe the effect of carbazole substitution on the redox and photophysical properties of this family of materials.

Results and Discussion

Synthesis of ligands and their iridium(III) complexes: The ligands are represented as CzFl$_n$Py, where Cz denotes *N*-hex-

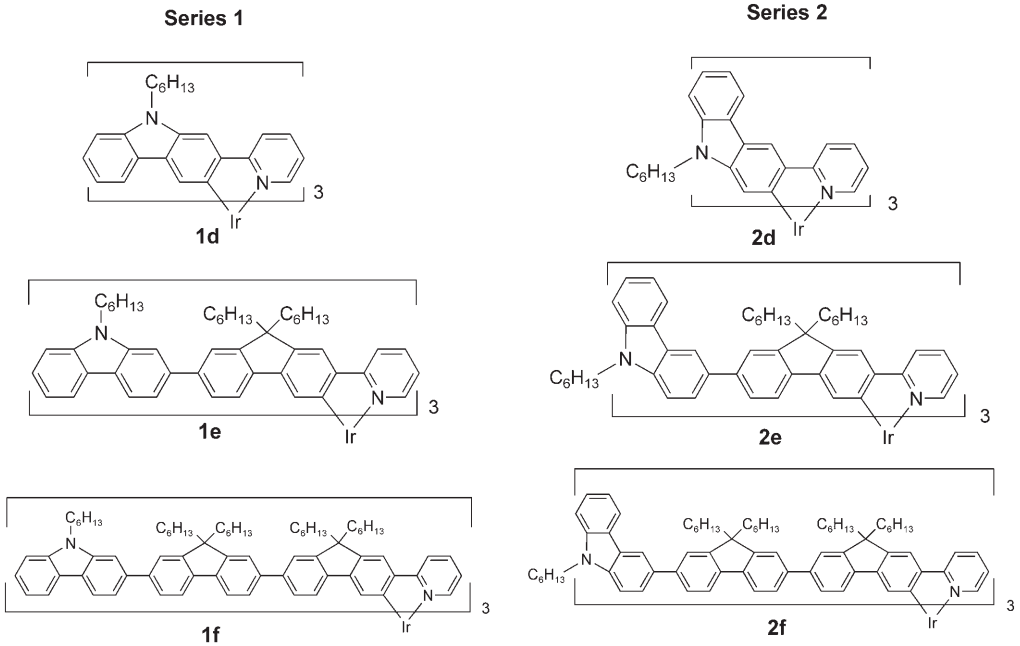

ylcarbazole, *n* equals the number of 9,9′-dihexylfluorene (Fl) units and Py is pyridine. In all cases, Py and Fl are substituted at the 2- and 2,7-positions, respectively, and carbazole moieties are substituted by either Py or Fl at the 2- or 3-positions, in series **1** and **2**, respectively. The key starting materials for ligands in both series **1** and **2** were the corresponding *N*-hexylcarbazol-2-yl and -3-yl boronic acids[15] **3** and **4**, and the bromo-(fluorenyl)$_{n=1,2}$-pyridine intermediates[16] **6** and **7** (Scheme 1). The ligands in series **1** and **2** were synthesized in good yields by the Suzuki–Miyaura cross-coupling reactions[17] of the corresponding carbazolylboronic acids **3** and **4** utilizing bromo compounds **5**, **6**, and **7**, as shown in Scheme 1. The detailed synthetic procedures and characterization data are given in the Supporting Information.

In these reactions, since bromo-(fluorenyl)$_{n=1,2}$-pyridine intermediates[16] **6** and **7** have very similar polarities to those of the ligands **1b–c** and **2b–c**, we opted to use an excess of the carbazolyl boronic acid due to its ease of removal from the crude product mixture and in order to force the reaction to completion. Trace amounts of unreacted free bromo-(fluorenyl)$_{n=1,2}$-pyridine intermediates **6** and **7** were successfully removed by repeated column chromatography.

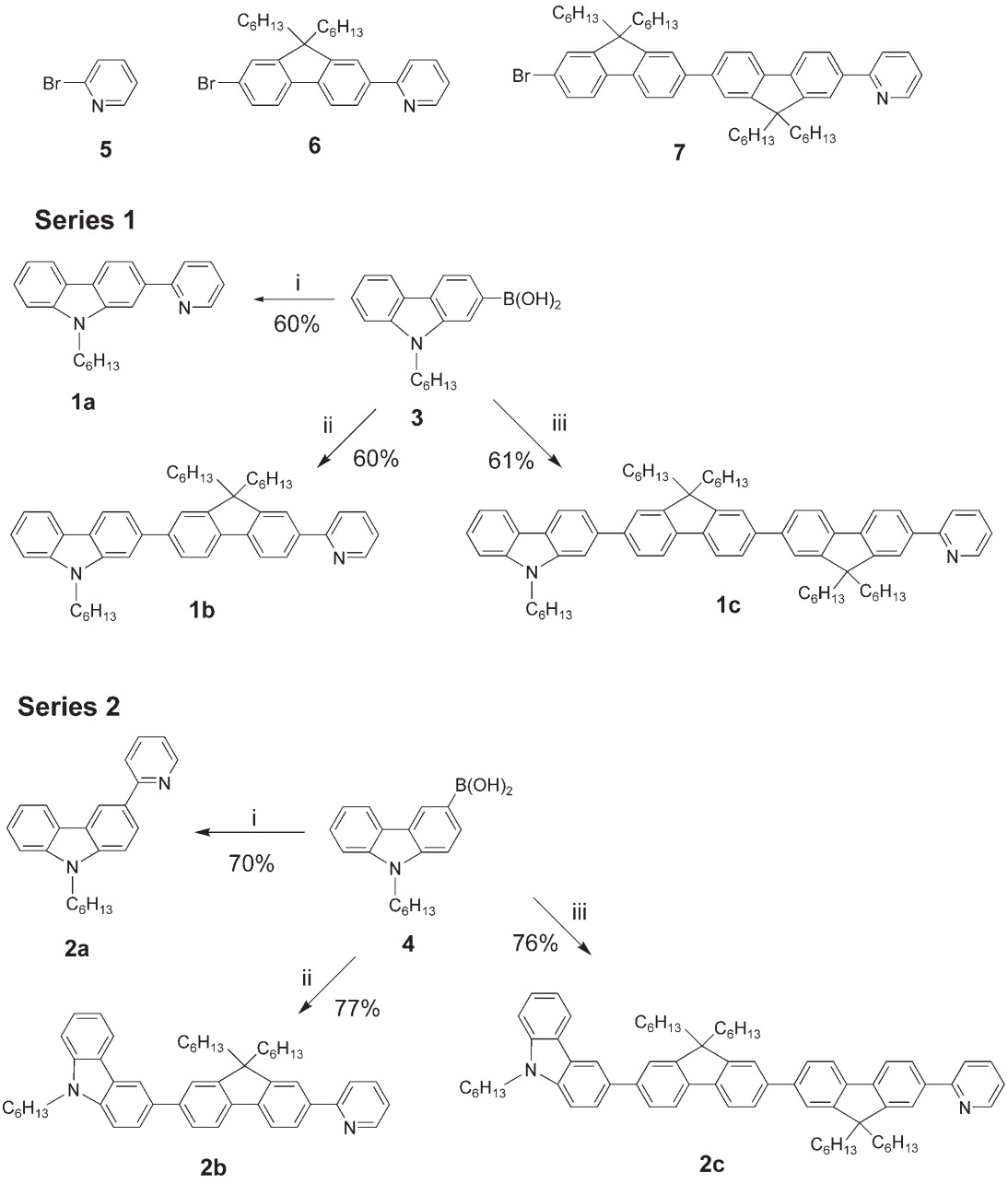

Scheme 1. Synthesis of ligands Cz-2-Fl$_n$Py **1a–c** and Cz-3-Fl$_n$Py **2a–c**. Reagents and conditions: i) **5**, [Pd(PPh$_3$)$_2$Cl$_2$], 2 M Na$_2$CO$_3$ (aq.), toluene, 90 °C, 20–40 h; ii) **6**, [Pd(PPh$_3$)$_4$] or [Pd(PPh$_3$)$_2$Cl$_2$], 2 M Na$_2$CO$_3$ (aq.), toluene, 90 °C, 50–60 h; iii) **7**, [Pd(PPh$_3$)$_4$] or [Pd(PPh$_3$)$_2$Cl$_2$], 2 M Na$_2$CO$_3$ (aq.), toluene, 90 °C, 50–60 h.

The triply cyclometalated iridium(III) complexes, **1d–f** (2-substituted) and **2d–f** (3-substituted) were prepared by reacting iridium(III) acetylacetonate, [Ir(acac)$_3$], with 1.7 equivalents of the corresponding cyclometalating ligand in glycerol at 220 °C for 48 h under an argon atmosphere[18] and were obtained in 4–60 % yields. The considerably higher yield for the 3-substituted complex **2d** (60 %) compared to that of the 2-substituted complex **1d** (20 %), may stem from the fact that the loss of a proton from the ligand **2a**, during the cyclometalating reaction, is further stabilized by the *meta*-positioned carbazole nitrogen in ligand **2a** compared to that in ligand **1a**. In addition to this, thermal gravimetric analysis showed that complex **1d** undergoes a 5 % by weight thermal decomposition at 196 °C indicating that there may be some loss of the complex during the cyclometalation at 220 °C. This is not unexpected for cyclometalation reactions such as these that utilize small ligands.[19] Each complex was unambiguously characterized by ^{1}H and ^{13}C NMR spectroscopy and MALDI-TOF mass spectrometry. The relative simplicity of the ^{1}H NMR spectra indicates that all the isolated complexes exist exclusively as the *fac* isomers around the Ir center.[18] The *fac* structure of **2d** was further confirmed by single-crystal X-ray analysis.[20] The MM3 optimized geometry of the *fac*-**2f** structure is shown in Figure 1.

Cyclic voltammetry: Cyclic voltammetric (CV) studies were carried out at 298 K using a Ag/AgNO$_3$ (CH$_3$CN) reference electrode and the ferrocene/ferrocenium couple[21] as a secondary reference. Dichloromethane solutions of the complexes containing 0.1 M tetra(*n*-butyl)ammonium hexafluorophosphate (*n*Bu$_4$NPF$_6$) as the supporting electrolyte were scanned at 100 mV s^{-1}. The CVs of all the complexes studied (**1d–f** and **2d–f**) display cleanly reversible oxidation potentials assigned to the metal-centered Ir^{III}/Ir^{IV} couple. The data for **1d–f** and **2d–f** are summarized in Table 1 and CV traces for all six complexes are shown in Figure SI-1. Owing to the electron-donating effect of the carbazole-nitrogen in the carbazole-2-pyridine ligand, where the nitrogen atom is *para* to the metalated Ir-phenyl center, the oxidation potential of **1d** ($E^{ox}_{1/2}$ = 0.14 V) is less positive (i.e. raised HOMO level) compared to that of **2d** ($E^{ox}_{1/2}$ = 0.30 V), where the carbazole-nitrogen atom is *meta* to the metalated Ir-phenyl center in the carbazole-3-pyridine.[22] The raised oxidation potential of the Ir^{III}/Ir^{IV} couple in both series with increasing ligand size is consistent with carbazole acting as a stronger electron donor than fluorene. A shielding effect of the core by the larger ligands may also contribute to raising the value of $E^{ox}_{1/2}$. This effect is most noticeable upon incorporation of the first fluorenyl unit. The positive shifts are 0.26 and 0.10 V in the sequence **1d**→**1e**→**1f**, and 0.70 and 0.50 V in the sequence **2d**→**2e**→**2f**.

The ligand-centered oxidations in the complexes (observed as two, three-electron waves) have more positive potentials than the Ir^{III}/Ir^{IV} couple and this is clearly exemplified by **2f** (Figure 1). The processes show good chemical reversibility and are electrochemically quasi-reversible[23] (especially the ligand waves); the current ratios for the three

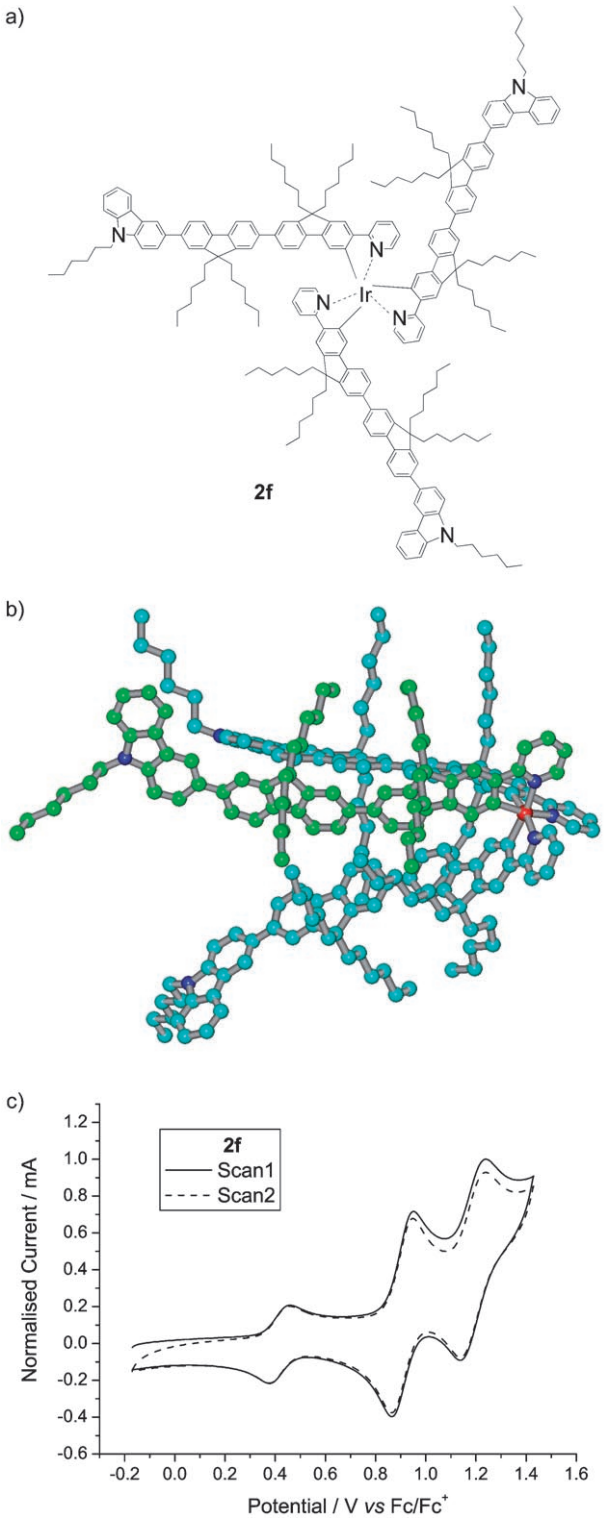

Figure 1. a) Molecule **2f** and b) the MM3-optimized geometry of the *fac* structure (color code: Ir red; N blue; C cyan (for two ligands) and green (for third ligand); hydrogen atoms are omitted for clarity). c) Cyclic voltammogram of **2f** in 0.1 M *n*Bu$_4$NPF$_6$ dichloromethane solution at 298 K, scan rate 100 mV s^{-1} (first two scan cycles shown). Scan 1: E^{ox}_{pa} 0.45, 0.95, 1.24; E^{ox}_{pc} 0.38, 0.86, 1.15 V.

oxidation waves reflect the metal-to-ligand ratio of 1:3. These complexes are, therefore, highly redox-active systems,

Table 1. Summary of the half-wave oxidation potentials for the Ir^{III}/Ir^{IV} couple ($E^{ox}_{1/2}$ [V]) obtained by cyclic voltammetry for complexes [Ir(Cz-2-$Fl_nPy)_3$] **1d–f** and [Ir(Cz-3-$Fl_nPy)_3$] **2d–f** and ferrocene versus Ag/$AgNO_3$.[a]

Complex	$E^{ox}_{1/2}$ [V]
[Ir(Cz-2-Py)$_3$] (**1d**)	+ 0.14
[Ir(Cz-2-Fl_1Py)$_3$] (**1e**)	+ 0.40
[Ir(Cz-2-Fl_2Py)$_3$] (**1f**)	+ 0.41
[Ir(Cz-3-Py)$_3$] (**2d**)	+ 0.30
[Ir(Cz-3-Fl_1Py)$_3$] (**2e**)	+ 0.37
[Ir(Cz-3-Fl_2Py)$_3$] (**2f**)	+ 0.42
ferrocene	+ 0.28

[a] 0.1 M (nBu$_4$NPF$_6$) in dichloromethane at 298 K, scan rate = 100 mV s^{-1}.

and the 7+ redox states are cleanly obtained within a readily-accessible potential window. Full experimental details, graphical illustrations (Figure SI-1 and SI-2) and additional CV data (Table SI-2) of the complexes and the free (uncomplexed) ligands are in the Supporting Information.

Differential scanning calorimetry (DSC) and thermal gravimetric analysis (TGA): The thermal properties of the complexes were also investigated by DSC and TGA. DSC analysis revealed that all of the complexes are amorphous solids, whose states are influenced by their ligand frameworks. For instance, **1d** exhibits no phase transition at all from 50 to 300 °C. This is in contrast to **1e** and **1f**, which first undergo crystallization at 170 °C and 221 °C, respectively, followed by broad melting transitions at 284 °C and 288 °C, respectively. On the other hand, complexes **2d** and **2f** show only a melting point at 297 °C (sharp) and 254 °C (broad), respectively, whereas **2e** undergoes crystallization at 91 °C, followed by a glass transition at 157 °C and melting at 281 °C (broad).

The TGA indicates that complexes **1e**, **1f**, **2d**, and **2f** exhibit good thermal stability with 5% weight loss temperatures ($\Delta T_{5\%}$) ranging from 399 °C to 410 °C. These $\Delta T_{5\%}$ values are similar to those reported for [Ir(ppy)$_3$] (ppy = 2-phenylpyridine) ($\Delta T_{5\%}$, = 413 °C).[24] However, complexes **1d** and **2e** have lower $\Delta T_{5\%}$ values at 196 °C and 270 °C, respectively. The DSC and TGA data are summarized in the Supporting Information in Table SI-2.

Solution-state photophysical properties

Absorption: The absorption spectra of complexes, [Ir(Cz-2-$Fl_nPy)_3$] **1d–f** and [Ir(Cz-3-$Fl_nPy)_3$] **2d–f**, in toluene are shown in Figure 2 and Figure 3, respectively. For all six complexes the strongest absorbance bands are assigned as $^1\pi$–π^* transitions that lie in the range $\lambda \sim 300$–400 nm. Overlapping these, the weaker absorptions above $\lambda \sim 400$ nm are assigned as singlet metal-to-ligand charge transfer (^{1}MLCT) transitions and at even longer wavelengths, absorption bands with much lower intensities are assigned as ^{3}MLCT bands. These assignments are made by analogy with previously reported Ir complexes[2,4a,b,6] and the calculations of Hay.[25] The absorption data for these complexes are summarized in Table SI-1. As illustrated in Figure 2 and Figure 3, by altering only

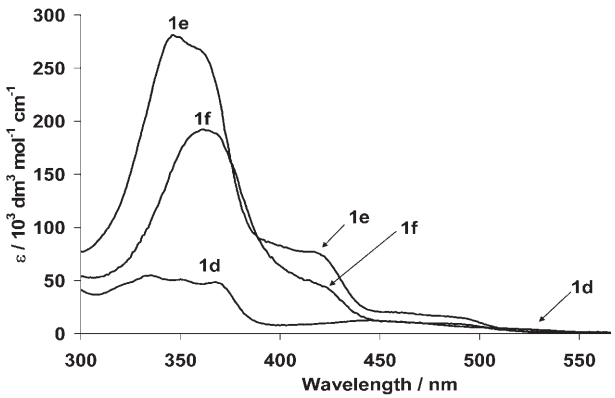

Figure 2. Absorbance spectra of complexes **1d–f** in toluene at 298 K.

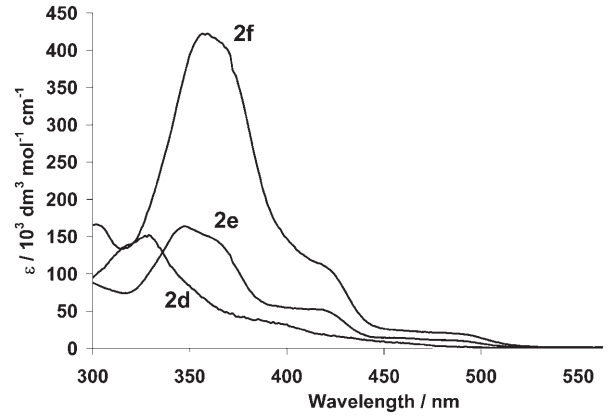

Figure 3. Absorbance spectra of complexes **2d–f** in toluene at 298 K.

the position of the pyridyl substitution on the carbazole unit from C-2 in **1d** to C-3 in **2d**, significantly different absorption spectra are observed. The C-3 substitution of the carbazole unit, which possesses a greater degree of electron-density in the HOMO,[9,10] as opposed to the 2-position, generates a higher energy ligand and hence blue-shifts the absorption bands for complex **2d**, compared to **1d**. Combined with this effect, for complex **1d** the carbazole nitrogen is positioned *para* to the metal center and can destabilize the ground state of the complex by electron-donation. The higher energy ground state, in relation to the unaltered excited state, contributes a red shift in the absorption bands for complex **1d**. The larger complexes **1e** and **1f**, when compared with their isomeric complexes **2e** and **2f**, respectively, show essentially identical absorption profiles over the range $\lambda = 300$–550 nm, but with significantly different ε values. Although the substitution of carbazole, when not directly bound to the metal center, has little effect on the spectral profile, the conjugation length on increasing from one fluorene unit in **1e** to two in **1f** (or from **2e** to **2f**) red shifts both the $^1\pi$–π^* transitions and MLCT bands (to a smaller extent) to lower energies.[26] Extinction coefficients (ε) are listed in Table SI-1 and are of the expected order of magnitude for these types of complexes.[2]

Emission: The degassed photoluminescence (PL) spectra for the [Ir(Cz-2-Fl$_n$Py)$_3$] **1d–f** and [Ir(Cz-3-Fl$_n$Py)$_3$] **2d–f** complexes in toluene are shown in Figure 4 and Figure 5, respectively. The emission intensities increase dramatically upon degassing but the spectral profiles remain unchanged. This is indicative of phosphorescent species which are susceptible to oxygen quenching.[4a,b] The emission maxima, λ_{max}, for these complexes are presented in Table 2 and range from 505 nm (**2d**) to 590 nm (**1d**). The most notable observation is the 85 nm difference in λ_{max} between complexes **1d** and **2d**. This is due to the Cz-substitution at the 2-position. Carbazole, when directly bound to the metal center, donates electrons from its nitrogen lone pair to the metal center via the *para*-position, raising the HOMO level and thus contributing to a red shift for **1d**. On the other hand, for complexes **1e–f** and **2e–f**, regardless of the Cz substitutions, when the number of fluorene units increases from one in **1e** and **2e** to two in **1f** and **2f**, only a small red-shift of 5 nm is observed, indicating a stabilization of the triplet states at 565 nm. This type of stabilization has been previously reported[16a,b] and occurs as the conjugation length increases. All the emission spectra show some degree of vibrational fine structure and this suggests that these complexes emit from a mixed ^{3}MLCT/$^3\pi$–π^* state.[18] Emission spectra for complexes **1d** and **2d** show the least vibrational fine structure. We suggest that due to the smaller ligands in **1d** and **2d** the ^{3}MLCT/$^3\pi$–π^* state contains less $^3\pi$–π^* character.[27] The Commission Internationale de L′Eclairage (CIE) chromaticity coordinates[28] for the spectra of the complexes in degassed toluene are listed in Table 2.

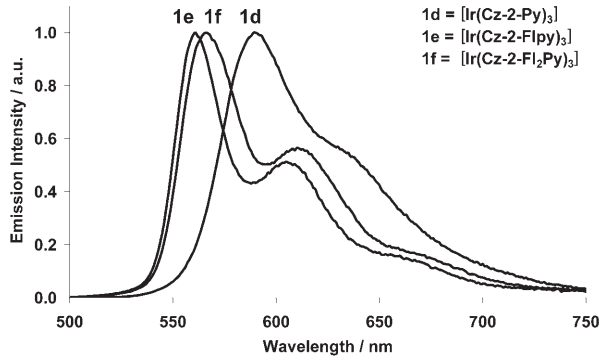

Figure 4. Normalized PL spectra for [Ir(Cz-2-Fl$_n$Py)$_3$] **1d–f** in degassed toluene at 298 K, $\lambda_{ex}=355$ nm.

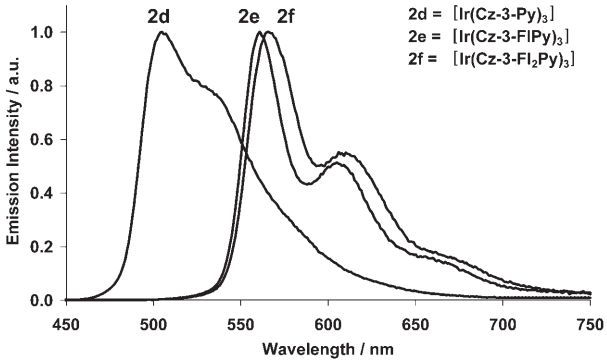

Figure 5. Normalized PL spectra for [Ir(Cz-3-Fl$_n$Py)$_3$] **2d–f** in degassed toluene at 298 K, $\lambda_{ex}=355$ nm.

Table 2. Summary of emission data for complexes **1d–f** and **2d–f** in degassed toluene at 298 K.

Degassed toluene	[Ir(Cz-2-Fl$_n$Py)$_3$]			[Ir(Cz-3-Fl$_n$Py)$_3$]		
	1d	**1e**	**1f**	**2d**	**2e**	**2f**
λ_{max}[a] [nm]	590	560	565	505	560	565
CIE coordinates						
x	0.63	0.55	0.57	0.25	0.54	0.57
y	0.37	0.45	0.43	0.64	0.46	0.43
τ_p[b] [μs]	3.2	4.8	7.4	1.9	4.4	6.6
Φ[c]	0.28	0.30	0.39	0.39	0.32	0.31

[a] $\lambda_{ex}=355$ nm, [b] $\lambda_{ex}=355$ nm, τ_p ±10% and [c] $\lambda_{ex}=450$ nm, Φ ±10%.

Phosphorescence lifetimes and photoluminescence quantum yields: Time-resolved luminescence decay measurements for the complexes (OD < 0.1 at $\lambda_{ex}=355$ nm) were performed at 298 K in degassed toluene. The emission was collected at λ_{max} for each complex and the phosphorescence decays were all found to follow first order kinetics. The solution-state phosphorescence lifetimes (τ_p) for complex series **1** are 3.2 μs (**1d**), 4.8 μs (**1e**) and 7.4 μs (**1f**), and for complex series **2** are 1.9 μs (**2d**), 4.4 μs (**2e**) and 6.6 μs (**2f**). The lifetimes increase with the size of the complexes (e.g. from 3.2 μs in [Ir(Cz-2-Py)$_3$] **1d** to 7.4 μs in [Ir(Cz-2-Fl$_2$Py)$_3$] **1f**). This indicates a weakening of the spin-orbit coupling and hence an increasing amount of $^3\pi$–π^* character in the lowest energy excited state, consistent with previously reported data[27] and our observation of vibrational fine structure in the emission spectra of the larger complexes (e.g. complexes **1e,f** and **2e,f**, Figure 4 and Figure 5).

The photoluminescence quantum yields (Φ) of the six complexes were recorded in degassed toluene at 298 K using *fac*-[Ir(ppy)$_3$] in degassed toluene as the standard ($\Phi=0.40$),[24,7b] $\lambda_{ex}=450$ nm. The Φ values obtained for the complexes in series **1** are 0.28 (**1d**), 0.30 (**1e**), and 0.39 (**1f**), and for complex series 2 are 0.39 (**2d**), 0.32 (**2e**), and 0.31 (**2f**), with ±10%. The Φ values are of the expected order of magnitude for these types of complexes.[2,4a,5b,16,18] The τ_p and Φ values are summarized in Table 2.

OLEDs: Preliminary studies have been made on devices with the following configuration: ITO/PEDOT:PSS/(PSBF:TAD):Ir complex/Ba/Al, all containing identical concentrations (2.44×10^{-3} M) of iridium guest in polyspirobifluorene:bis(triphenyl)diamine (PSBF:TAD) copolymer host.[29] The structure of the PSBF:TAD copolymer is shown in the Supporting Information. Figure 6 shows the normalized electroluminescence (EL) spectra of devices containing solely the PSBF:TAD copolymer and the PSBF:TAD copolymer devices doped with [Ir(Cz-2-Py)$_3$] (**1d**) and [Ir(Cz-3-Py)$_3$] (**2d**).

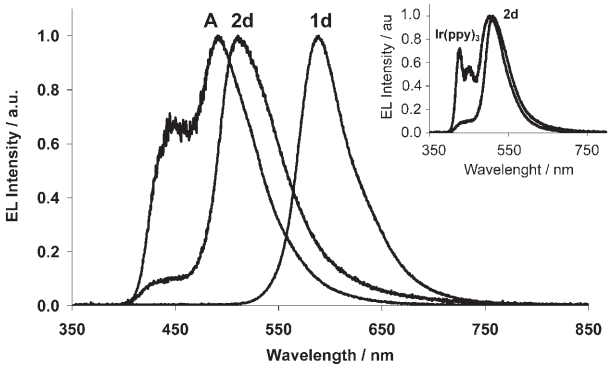

Figure 6. Normalized electroluminescence spectra of the PSBF:TAD copolymer host (**A**), [Ir(Cz-2-Py)$_3$] (**1d**) and [Ir(Cz-3-Py)$_3$] (**2d**) and inset the normalized EL spectra of [Ir(Cz-3-Py)$_3$] (**2d**) and *fac*-[Ir(ppy)$_3$] under the same conditions. Note the presence of host emission (peaks at 420–450 nm) for devices containing [Ir(Cz-3-Py)$_3$] (**2d**) and especially *fac*-[Ir(ppy)$_3$].

The EL spectrum of complex **1d** (λ_{max} 590 nm) is the same as observed in solution PL; however, for complex **2d** the λ_{max} value for the EL (500 nm) is blue-shifted by 5 nm compared to its PL. This is most likely due to emission from both the host and guest species (**2d**). The lower energy shoulders seen in the solution PL spectra of **1d** and **2d** (Figure 4 and Figure 5), which are typical of vibrational energy levels of mixed MLCT/π–π* transitions, are diminished in the solid-state matrix device environment (Figure 6), giving rise to narrower EL bands and hence purer colors.

For a comparison, devices doped with *fac*-[Ir(ppy)$_3$] (*fac*-[tris(2-phenylpyridine)iridium(III)]) were also prepared under identical conditions, the EL of which is depicted together with that of [Ir(Cz-3-Py)$_3$] (**2d**) in Figure 6 (inset). Both the devices containing **2d** and *fac*-[Ir(ppy)$_3$] show host emission (Figure 6, inset: shoulders/peaks at about 420–450 nm), but to a considerably greater extent with *fac*-[Ir(ppy)$_3$]. This is an unusual EL spectrum for *fac*-[Ir(ppy)$_3$] compared to the standard EL spectrum obtained after thermal treatment (Figure SI-4) and could result from aggregate formation. The increased solubility of **1d** and **2d** imparted by the *N*-hexyl chains would diminish this effect by facilitating homogeneous film formation.

In addition to this advantageous solubility effect, under the same doping levels, the 3-substituted carbazole unit in **2d** may enhance charge trapping, hence maintaining the green color of the emitted light. In marked contrast, the device containing **1d** is an orange emitter. The striking difference in color between **1d** and **2d** is a consequence of the electron donating ability of the carbazole unit in complex **1d** (enhanced by the 2-substituted Cz unit placing the nitrogen atom *para* to the Ir center). The CIE coordinates of the devices are as follows: **1d** ($x=0.58$, $y=0.39$) and **2d** ($x=0.22$, $y=0.60$) compared to *fac*-[Ir(ppy)$_3$] ($x=0.35$, $y=0.60$) as reported by Yang et al.[30] and are shown on a color CIE diagram in the Supporting Information.

The current–voltage (I–V) characteristics of the doped devices are shown in Figure 7, where [Ir(Cz-2-Py)$_3$] (**1d**) has the higher turn-on voltage (≈4 V) and lower device conductivity (167 mA cm^{-2} at 7 V). This indicates a greater degree of exciton trapping for complex **1d**, compared to complex **2d**, due to the presence of the lower energy triplet excited states as also indicated by the PL and EL spectra in Figure 4 and Figure 6, respectively. This is reflected by the higher emission intensity (luminance) (4354 cd m^{-2}) for complex [Ir(Cz-2-Py)$_3$] (**1d**; Figure 7,inset) and the higher external quantum efficiency (1.3 %), shown in Figure 8.

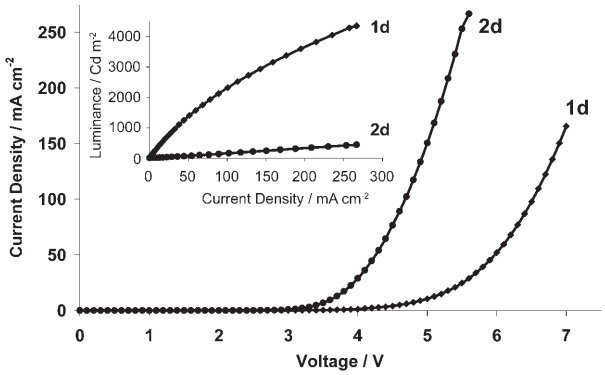

Figure 7. Current density (mA cm^{-2}) versus voltage (V) and inset the luminance (Cd m^{-2}) versus current density (mA cm^{-2}) for the devices containing [Ir(Cz-2-Py)$_3$] (**1d**) and [Ir(Cz-3-Py)$_3$] (**2d**).

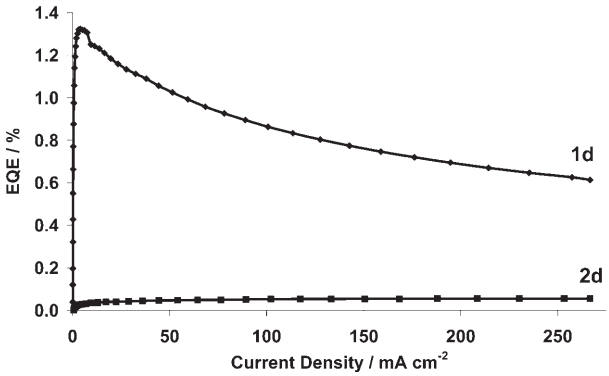

Figure 8. The external quantum efficiency (EQE) versus current density (mA cm^{-2}) for the devices containing [Ir(Cz-2-Py)$_3$] (**1d**) and [Ir(Cz-3-Py)$_3$] (**2d**).

The lower turn-on voltage (≈3 V) and the higher device conductivity (267 mA cm^{-2} at 5.6 V) for [Ir(Cz-3-Py)$_3$] (**2d**) indicate that the holes and electrons are passing into the active layer without forming excitons—this is partly due to the lower trapping efficiency. As a consequence a low exciton population is generated inside the active layer, yielding a low luminance (437 cd m^{-2}) and low EQE (0.06 %) for this device. Furthermore, the low lying triplet level of the host polymer will act to quench excitons on the [Ir(Cz-3-Py)$_3$]

(**2d**) dopant via energy transfer, further reducing the EQE. To optimize the performance of the [Ir(Cz-3-Py)$_3$] dopant, a high triplet energy host material is required to avoid this quenching mechanism. The EL spectra of the devices (color purity and intensity) remained unchanged at 6 V (current density, 100 mA cm^{-2}) with the time to half brightness of 9 ± 3 h (variation from device to device) under continuous operation with no change in the spectral profile, confirming the high chemical stability of complexes. Detailed studies on the effect of varying device thickness, doping concentration and the use of additional blocking layers etc. would be expected to enhance performance. Encapsulation could further improve the durability of the devices.

Conclusions

We have synthesized two new series of ligands **1a–c** and **2a–c**, respectively, of the type Cz-Fl$_n$Py (n = 0, 1, 2) which possess carbazole moieties bonded at the C-2 and C-3 positions, and obtained their corresponding homoleptic tris-cyclometalated complexes *fac*-[Ir(Cz-2-Fl$_n$Py)$_3$] **1d–f** and [Ir(Cz-3-Fl$_n$Py)$_3$] **2d–f**, which are solution-processible triplet emitters. For complexes **1d** and **2d**, in which the Cz moiety is bonded directly to the metal center, on changing the Cz substitution from C-2 to C-3, marked changes are seen in the solution-state photophysical data: namely an 85 nm blue-shift in emission, a decrease in the luminescence lifetime and an increase in the PLQY value. However, for complexes **1e,f** and **2e,f**, where the carbazole unit is not directly bonded to the metal center, the effect of changing from C-2 to C-3 substitution is greatly diminished. We have established that carbazole-based iridium complexes are suitable dopants for OLEDs with turn-on voltages of about 3–4 V. The marked difference in performance between the devices containing complexes **1d** and **2d** is attributed to the relative degree of energy transfer between the host and guest species. The device containing complex [Ir(Cz-2-Py)$_3$] (**1d**) has an emission peak at λ_{max} = 590 nm, an EQE of 1.3%, and an emission intensity (luminance) of 4354 Cd m^{-2}, which is comparable to devices utilizing electrophosphorescent polymers containing carbazole moieties.[12a] Future work will involve fine-tuning of the chemical structure and photophysical properties of pyridine-carbazole-fluorene hybrid species by adapting the synthetic strategies described herein. Particularly interesting targets will be cyclometalated Py-Cz-X arrays (X = (Fl)$_n$ or (Cz)$_n$ n = 1–3). Additionally we will use different host materials (e.g. a host possessing a higher triplet energy for [Ir(Cz-3-Py)$_3$] (**2d**)) to build on the promising results reported in this article and to probe deeper into the fundamental properties of this fascinating class of materials.

Acknowledgements

We thank Durham County Council (Project SP/082), CENAMPS and the University of Durham Photonic Materials Institute for funding this work.

[1] a) Y. Shirota, *J. Mater. Chem.* **2005**, *15*, 75–93; b) A. C. Grimsdale, K. Müllen, *Angew. Chem.* **2005**, *117*, 5732–5772; *Angew. Chem. Int. Ed.* **2005**, *44*, 5592–5629.
[2] V. V. Grushin, N. Herron, D. D. LeCloux, W. J. Marshall, V. A. Petrov, Y. Wang, *Chem. Commun.* **2001**, 1494–1495.
[3] a) S. Lamansky, P. I. Djurovich, D. Murphy, F. Abdel-Razzaq, R. C. Kwong, I. Tysba, M. Bortz, B. Mui, R. Bau, M. E. Thompson, *Inorg. Chem.* **2001**, *40*, 1704–1711; b) C. Adachi, M. A. Baldo, S. R. Forrest, S. Lamansky, M. E. Thompson, R. C. Kwong, *Appl. Phys. Lett.* **2001**, *78*, 1622–1624; c) J. Nishida, H. Echizen, T. Iwata, Y. Yamashita, *Chem. Lett.* **2005**, 1378–1379.
[4] a) P. Coppo, E. A. Plummer, D. De Cola, *Chem. Commun.* **2004**, 1774–1775; b) J. C. Ostrowski, M. R. Robinson, A. J. Heeger, G. C. Bazan, *Chem. Commun.* **2002**, 784–785.
[5] a) A. Beeby, S. Bettington, I. D. W. Samuel, Z. Wang, *J. Mater. Chem.* **2003**, *13*, 80–83; b) S. Jung, Y. Kang, H.-S. Kim, Y.-H. Kim, C.-L. Lee, J.-J. Kim, S.-K. Lee, S.-K. Kwon, *Eur. J. Inorg. Chem.* **2004**, 3415–3423; c) B. Liang, C. Jiang, Z. Chen, X. Zhang, H. Shi, Y. Cao, *J. Mater. Chem.* **2006**, *16*, 1281–1286.
[6] a) Md. K. Nazeerudin, R. Humphry-Baker, D. Berner, S. Rivier, L. Zuppiroli, M. Graetzel, *J. Am. Chem. Soc.* **2003**, *125*, 8790–8797; b) C. Lee, R. R. Das, J. Kim, *Chem. Mater.* **2004**, *16*, 4642–4646; c) J. Li, P. I. Djurovich, B. D. Alleyne, M. Yousufuddin, N. N. Ho, J. C. Thomas, J. Peters, R. Bau, M. E. Thompson, *Inorg. Chem.* **2005**, *44*, 1713–1727.
[7] a) S. Lamansky, P. Djurovich, D. Murphy, F. Abdel-Razzaq, H.-E. Lee, C. Adachi, P. E. Burrows, S. R. Forrest, M. E. Thompson, *J. Am. Chem. Soc.* **2001**, *123*, 4304–4312; b) I. R. Laskar, T.-M. Chen, *Chem. Mater.* **2004**, *16*, 111–117; c) Review: E. Holder, B. M. W. Langeveld, U. S. Schubert, *Adv. Mater.* **2005**, *17*, 1109–1121; d) *Organic Electroluminescence*, (Ed.: Z. H. Kakafi), CRC, Boca Raton, **2005**.
[8] a) J. P. J. Markham, E. B. Namdas, T. D. Anthopoulos, I. D. W. Samuel, G. J. Richards, P. L. Burn, *Appl. Phys. Lett.* **2004**, *85*, 1463–1465; b) X. H. Yang, D. Neher, *Appl. Phys. Lett.* **2004**, *84*, 2476–2478; c) X. H. Yang, F. Jaiser, S. Klinger, D. Neher, *Appl. Phys. Lett.* **2006**, *88*, 021107.
[9] J. Huang, Y. Niu, W. Yang, Y. Mo, M. Yuan, Y. Cao, *Macromolecules* **2002**, *35*, 6080–6082.
[10] a) J.-F. Morin, M. Leclerc, *Macromolecules* **2002**, *35*, 8413–8417; b) J.-F. Morin, N. Drolet, Y. Tao, M. Leclerc, *Chem. Mater.* **2004**, *16*, 4619–4626; c) S. Wakim, J. Bouchard, N. Blouin, A. Michaud, M. Leclerc, *Org. Lett.* **2004**, *6*, 3413–3416.
[11] a) K. Brunner, A. van Dijken, H. Börner, J. J. A. M. Bastiaansen, N. M. M. Kiggen, B. M. W. Langeveld, *J. Am. Chem. Soc.* **2004**, *126*, 6035–6042; b) A. van Dijken, J. J. A. M. Bastiaansen, N. M. M. Kiggen, B. M. W. Langeveld, C. Rothe, A. Monkman, I. Bach, P. Stossel, K. Brunner, *J. Am. Chem. Soc.* **2004**, *126*, 7718–7727; c) for a non-conjugated carbazole-fluorene host material see: K.-T. Wong, Y.-M. Chen, Y.-T. Lin, H.-C. Su, C. Wu, *Org. Lett.* **2005**, *7*, 5361–5364.
[12] a) H. Zhen, C. Jiang, W. Yang, J. Jiang, F. Huang, Y. Cao, *Chem. Eur. J.* **2005**, *11*, 5007–5016; b) J. Jiang, C. Jiang, W. Yang, H. Zhen, F. Huang, Y. Cao, *Macromolecules* **2005**, *38*, 4072–4080; c) C. S. M. Mak, A. Hayer, S. I. Pascu, S. E. Watkins, A. B. Holmes, A. Köhler, R. H. Friend, *Chem. Commun.* **2005**, 4708–4710; d) Z. Liu, M. Guan, Z. Bian, D. Nie, Z. Gong, Z. Li, C. Huang, *Adv. Funct. Mater.* **2006**, *16*, 1441–1448.
[13] a) T. Tsuzuki, N. Shirasawa, T. Suzuki, S. Tokito, *Jpn. J. Appl. Phys. Part 1* **2005**, *44*, 4151–4154; b) E. B. Namdas, A. Ruseckas, I. D. W. Samuel, S.-C. Lo, P. L. Burn, *Appl. Phys. Lett.* **2005**, *86*, 091104.
[14] a) S. Igawa, T. Takiguchi, A. Kamatani, S. Okada, A. Tsuboyama, K. Miura, T. Moriyama, H. Iwawaki, Patent No. JP 03/342284, **2002**; b) R. Zhu, J. Lin, G.-A. Wen, S.-J. Liu, J.-H. Wan, J.-C. Feng, Q.-L. Fan, G.-Y. Zhong, W. Wei, W. Huang, *Chem. Lett.* **2005**, 1668–1669.
[15] M. Tavasli, S. Bettington, M. R. Bryce, A. S. Batsanov, A. P. Monkman, *Synthesis* **2005**, 1619–1624.

[16] a) M. Tavasli, S. Bettington, M. R. Bryce, H. Al Attar, F. B. Dias, S. King, A. P. Monkman, *J. Mater. Chem.* **2005**, *15*, 4963–4970; b) for analogous (fluorenyl)$_n$-phenylpyridine ligands see: A. J. Sandee, C. K. Williams, N. R. Evans, J. E. Davies, C. E. Boothby, A. Köhler, R. H. Friend, A. B. Holmes, *J. Am. Chem. Soc.* **2004**, *126*, 7041–7048.
[17] N. Miyaura, A. Suzuki, *Chem. Rev.* **1995**, *95*, 2457–2483.
[18] A. B. Tamayo, B. D. Alleyne, P. I. Djurovich, S. Lamansky, I. Tsyba, N. N. Ho, R. Bau, M. E. Thompson, *J. Am. Chem. Soc.* **2003**, *125*, 7377–7387.
[19] K. Dedeian, P. I. Djurovich, F. O. Garces, G. Carlson, R. J. Watts, *Inorg. Chem.* **1991**, *30*, 1685–1687.
[20] See the Supporting Information. CCDC-260851 (**2d**) contains the supplementary crystallographic data for this paper. These data can be obtained free of charge from The Cambridge Crystallographic Data Centre via www.ccdc.cam.ac.uk/data_request/cif.
[21] N. G. Connelly, W. E. Geiger, *Chem. Rev.* **1996**, *96*, 877–910.
[22] During the course of our work, similar effects on redox potentials were reported by Yamashita et al. for a series of bis-cyclometalated Ir^{III} complexes based on phenylpyridines substituted with a diphenylamino group: see ref. [3c].
[23] Chemical reversibility was established by only very minor changes in the peak potentials and current for each wave on repeated cycling. Electrochemical reversibility is defined as i) the ratio between the cathodic and anodic peak current $I_c/I_a \approx 1.0$; ii) the peak potentials E_p were independent of the scan rate; iii) $\Delta E_p \approx (59/z)$ mV, where z is the number of electrons involved in the process.
[24] A. Tsuboyama, H. Iwawaki, M. Furugori, T. Mukaide, J. Kamatani, S. Igawa, T. Moriyama, S. Miura, T. Takiguchi, S. Okada, M. Hoshino, K. Ueno, *J. Am. Chem. Soc.* **2003**, *125*, 12971–12979.
[25] P. J. Hay, *J. Phys. Chem. A* **2002**, *106*, 1634–1641.
[26] A similar red shift is observed in oligo(fluorenyl) chains: A. L. Kanibolotsky, R. Berridge, P. J. Skabara, I. F. Perepichka, D. C. C. Bradley, M. Koeberg, *J. Am. Chem. Soc.* **2004**, *126*, 13695–13702.
[27] P. J. Spellane, R. J. Watts, *Inorg. Chem.* **1993**, *32*, 5633–5636.
[28] R. W. Burnham, R. M. Hanes, C. J. Bartleson, *Color: A Guide to Basic Facts and Concepts, Vol. 6*, Wiley, Chichester, **1967**, pp. 123–150.
[29] C. Rothe, H. A. Al Attar, A. P. Monkman, *Phys. Rev. B* **2005**, *72*, 155330.
[30] C.-H. Yang, K.-H. Fang, C.-H. Chen, I.-W. Sun, *Chem. Commun.* **2004**, 2232–2233.

Received: August 22, 2006
Published online: November 8, 2006

